Cells in human postmortem brain tissue slices remain alive for several weeks in culture

RONALD W. H. VERWER,*[,1] WIM T. J. M. C. HERMENS,* PAUL A. DIJKHUIZEN,*[,2] OLIVIER TER BRAKE,* ROBERT E. BAKER,* AHMAD SALEHI,*[,3] ARJA A. SLUITER,* MARLOES J. M. KOK,* LINDA J. MÜLLER,[†] JOOST VERHAAGEN,* AND DICK F. SWAAB*

Graduate School Neurosciences Amsterdam, *Netherlands Institute for Brain Research, and [†]Netherlands Ophthalmic Research Institute, 1105 AZ Amsterdam, The Netherlands

ABSTRACT **Animal models for human neurological and psychiatric diseases only partially mimic the underlying pathogenic processes. Therefore, we investigated the potential use of cultured postmortem brain tissue from adult neurological patients and controls. The present study shows that human brain tissue slices obtained by autopsy within 8 h after death can be maintained in vitro for extended periods (up to 78 days) and can be manipulated experimentally. We report for the first time that *1)* neurons and glia in such cultures could be induced to express the reporter gene LacZ after transduction with adeno-associated viral vectors and *2)* cytochrome oxidase activity could be enhanced by the addition of pyruvate to the medium. These slice cultures offer new opportunities to study the cellular and molecular mechanisms of neurological and psychiatric diseases and new therapeutic strategies.—Verwer, R. W. H., Hermens, W. T. J. M. C. Dijkhuizen, P. A., ter Brake, O., Baker, R. E., Salehi, A., Sluiter, A. A., Kok, M. J. M., Müller, L. J., Verhaagen, J., Swaab, D. F. Cells in human postmortem brain tissue slices remain alive for several weeks in culture. *FASEB J.* 16, 54–60 (2002)**

Key Words: aging · Alzheimer's disease · human brain · tissue culture · transgene expression

BRAIN DISORDERS ARE complex diseases often associated with multiple genetic, environmental, and age-related risk factors (1–5). Although animal models have contributed greatly to our understanding of human neurodegenerative diseases, they often fall short of mirroring the full range of symptoms associated with the human condition (6, 7). This may be partly due to the complex nature of neurodegenerative disorders. Some aspects may be unique for humans and therefore cannot be investigated in animal models. Although ethical and practical considerations favor the use of human autopsy brain tissue as opposed to biopsy material, it is generally thought that such tissue is not suitable for experimentation due to the deleterious effects of agonal state at death and postmortem delay on labile cellular constituents (8). However, we have recently shown that anatomical connections can be traced in human postmortem brain tissue during the first 24 h in vitro due to the capacity of cells to continue active axonal and dendritic transport (9). Moreover, studies by other groups have shown that it is possible to culture dissociated neurons or minced brain slices from adult postmortem rats and humans (10–15). These latter studies, however, did not include experimental manipulations. In the present study, we used organotypic cultures to show that many cells in postmortem adult human central nervous system (CNS) tissue remain viable for long periods and can be manipulated experimentally.

MATERIALS AND METHODS

Patients

The data presented in this report are based on material from control (C, n=9), Alzheimer (AD, n=13), Parkinson (PD, n=3), multiple sclerosis (MS, n=2), Lewy body (LBD, n=1), non-Alzheimer dementia (NAD, n=1), and Pick (PID, n=1) patients. The control subjects had no primary neurological or psychiatric disease. Permission was obtained for performing the brain autopsy and the use of tissues and medical information for the culturing purposes from the Ethical Committee of the Medical Faculty of the Free University (Amsterdam, The Netherlands) where the autopsies were performed in the framework of the Netherlands Brain Bank. The age of the patients ranged from 45 to 93 (mean: 79 years; SD: 13 years). Postmortem delays varied between 2 and 8 h (mean: 4.2 h; SD: 1.2 h). The agonal state at death was assessed using the pH of the cerebrospinal fluid (16, 17). During the postmortem delay, the bodies of the patients were transported to the autopsy room at ambient temperature, which has been shown to be compatible with neuronal survival after cardiac arrest in rodents (15, 18).

Culture conditions and histochemical and immunocytochemical staining procedures

At autopsy, one to six tissue slabs were dissected from the motor cortex by making incisions perpendicular to the lon-

[1] Correspondence: Netherlands Institute for Brain Research, Meibergdreef 33, 1105 AZ Amsterdam, The Netherlands. E-mail: r.verwer@nih.knaw.nl

[2] Present address: Department of Neuroscience, Johns Hopkins University School of Medicine, Baltimore, MD, USA.

[3] Present address: Department of Neurology and Neurological Sciences, Stanford University Medical Center, Stanford, CA, 94034-5489 USA.

0892-6638/02/0016-0054 © FASEB

gitudinal axis of the gyrus. The slabs (~0.5 cm thick with a surface of ~2 cm×2 cm) were transported to the culture facilities in capped tubes containing 10 ml Hank's basic salts solution (Life Technologies, Breda, The Netherlands) with 6 mg/ml glucose, 10 mM HEPES buffer, and 50 μg/ml gentamicin (room temperature). The slabs were cut in half so that two rods of sulcus-facing cortex were obtained. These rods were chopped yielding 20–40 slices (average size ~3 mm×4 mm×0.2 mm), which contained all cortical layers and a part of the white matter. The time needed for transport and preparation of the slices generally ranged between 1 and 2 h. The slices were cultured free-floating in uncoated 24-wells plates (Life Technologies) with 1–4 slices/well in 500 μl chemically defined medium (R16; 19) buffered by 10 mM HEPES. The slices were systematically allocated to experimental blocks (treatment, time in vitro, etc.) to exclude the influence of differences between the slabs. The cultures were kept at 35°C, with constant humidity and 95% air and 5% CO_2. In some experiments, the basal medium was supplemented with neurotrophic factors or pyruvate. Neurotrophic factors (Alomone Labs, Jerusalem, Israel) were added as a mixture containing 5 ng/ml nerve growth factor (NGF), 5 ng/ml brain derived neurotrophic factor (BDNF), and 10 ng/ml neurotrophin-3 (NT-3). Three times a week, 100 μl medium was replaced by fresh medium containing all the appropriate additives. For evaluation of neuropathological hallmarks and histological characterization, slices were fixed with 4% formaldehyde in phosphate-buffered saline (PBS, pH 7.4). Standard immunocytochemical staining procedures included antibodies to β-amyloid (DAKO, Glostrup, Denmark), 1:200; abnormally phosphorylated tau (AT-8, Immunogenetics, Zwijndrecht, Belgium), 1:300; neuronal nuclear protein (NeuN, Chemicon, Temecula, CA), 1:100; glial fibrillary acidic protein (GFAP, DAKO), 1:400, and human leukocyte antigen (HLA-DP,DQ,DR, DAKO), 1:100. Secondary antibodies (Vector Laboratories, Burlingame, CA or Jackson, West Grove, PA) were either conjugated with horseradish peroxidase (HRP) or biotin. Slices treated with biotinylated secondary antibodies were subsequently incubated with avidin-biotin complex conjugated with HRP (Elite ABC kit, Vector Laboratories) 1:800 or streptavidin-β-galactosidase (Roche, Mannheim, Germany) 1:1000. HRP conjugated reagents were visualized with 0.025% 3,3′-diaminobenzidine (DAB). Between incubations, the slices were rinsed 3 × 10 min with Tris-buffered saline (pH 7.6). Before detection of β-galactosidase, slices were washed three times with PBS and incubated at 37°C with 0.4 mg/ml 5-bromo-4-chloro-3-indolyl-β-galactopyranoside (X-gal, Life Technologies), 5 mM K_3ferricyanide, 5 mM K_2ferrocyanide, 2 mM $MgCl_2$ in PBS. Cells were traced by application of very small crystals of the carbocyanine dye DiI (Molecular Probes, Eugene, OR) to formaldehyde fixed slices (n=21) from three patients. Slices from two patients (one control, one AD) were processed according to standard electron microscopy protocols using a sucrose based fixative to preserve the extracellular space (20).

Viability of the slices was evaluated using the Live/Dead kit (L-3224, calcein-AM and ethidium homodimer-1; Molecular Probes) according to the protocol supplied by the manufacturer. A Zeiss 410 Invert confocal laser scanning microscope (CLSM) (lasers: argon, 488 nm; helium-neon, 543 nm) was used for visual inspection and photography of the viability preparations. Within 5–10 μm of the slice surfaces, only cell debris was present; therefore, CLSM pictures were taken at least 5–10 μm from either surface.

Cytochrome oxidase activity was determined using DAB histochemistry (21), which has been shown to correlate well with spectrophotometrical assessment (22). Specificity of the cytochrome oxidase activity staining was validated using 0.06% sodium azide.

Transduction with recombinant AAV vectors

Recombinant adeno-associated virus (rAAV) containing the reporter gene for *Escherichia coli* β-galactosidase (LacZ) was produced as described previously (23). The transgene-expressing unit titer (tu/ml) of the virus stocks was determined by coinfection of 293 cells with dilutions of the rAAV vector and adenovirus (*Ad*(dl309), multiplicity of infection of 3) (23). For rAAV infections, 4–10 slices/well were incubated overnight in 100 μl medium with $1 \times 10^7 \times 10^8$ tu/ml. Subsequently, the slices were redistributed over wells with fresh medium such that each well contained two or three slices. One to 14 days after infection, the slices were fixed briefly with 4% formaldehyde in PBS. The presence of β-galactosidase was detected as described above.

Quantitative analysis

Estimates of the number of viable cells in the cortical layers of the slices were obtained from systematic random sampled CLSM images (16–30 images/slice; 4 slices/time point/patient) made with a 25× oil objective. A counting frame containing 12 quadrants (20×20 μm) with exclusion and inclusion lines (24) was superimposed over each image. Each cell whose nucleus was completely or partially within the counting frame without touching an exclusion line was scored in either of three categories: *1)* viable: green cytoplasm with a dark nucleus, *2)* leaky: green cytoplasm with a red nucleus, or *3)* dead: a red nucleus without a discernible cytoplasm. The mean height of the nuclei was determined to correct for shape distortion in the direction of the z axis (25) and provide volumetric density estimates.

The overall cytochrome oxidase activity was quantified by measuring the mean optical density per area of the precipitated DAB with an automated image analysis system (IBAS-Kontron, Eching, Germany) as described previously (26). For viability data, we used analysis of variance and for the cytochrome oxidase activity data linear mixed effects models (27) as provided by the S-PLUS 2000 software (Insightful Inc., Seattle, WA).

RESULTS

In most experiments, motor cortex slices were maintained in culture for periods ranging from 1 to 50 days. In exceptional cases (n=2), such slices were maintained for up to 78 days in vitro (DIV 78). For histological characterization and evaluation of pathological hallmarks, several slices from each patient were fixed at DIV 0 with 4% formaldehyde PBS and subsequently immunostained with various antibodies. Motor cortex slices from Alzheimer (AD) patients and a Lewy body disease patient exhibited mild to strong AD pathology. Cortical tissue from only one AD patient showed no signs of pathology in the motor cortex. Motor cortex slices from patients diagnosed as control, PD, PID, or MS exhibited at most very mild neuropathology. As was clear from the histological and the electron microscopic preparations made later, the slices retained their typical structural features after long periods in vitro (**Fig. 1*A–F***). Cell populations of the cultured slices included neurons, astrocytes, and microglia (Fig. 1*B–D*). Neurons still possessed apical and basal dendrites

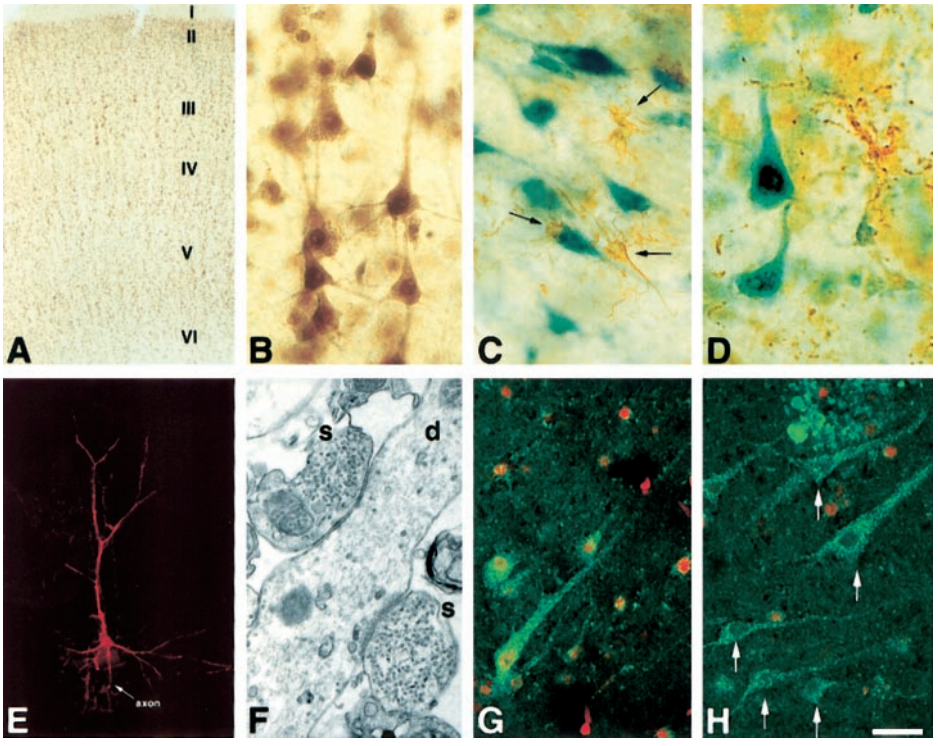

Figure 1. Histology and viability staining of motor cortex slices after long-term culturing. *A)* Overview of the cortical layers in a slice at DIV 25 (NeuN; Alzheimer patient, 99–139). *B)* Detail of layer III pyramidal neurons at DIV 38 (NeuN; control patient, 00–090). *C)* Astrocytes in layer III at DIV 78 (control, 00–090) stained with an antibody to GFAP (brown) and counterstained with NeuN (green). GFAP and NeuN were visualized using peroxidase (DAB) and β-galactosidase (X-gal), respectively. *D)* Microglial cells (HLA, brown) and neurons (NeuN, green) in layer III at DIV 78 (control, 00–090). *E)* DiI tracing reveals the extensive dendritic arborizations of an upper layer III pyramidal neuron at DIV 50 (non-Alzheimer dementia patient, 99–142). This figure is composed of 2 optical CLSM sections that were taken 20 μm apart. *F)* Electron micrograph showing axodendritic synapses at DIV 25 (AD, 99–139). *G)* Viability staining of a motor cortex slice (layer III) kept in basal medium (R16) for 48 days (AD, 99–139). *H)* Viability staining of a motor cortex slice (layer III) kept in basal medium (R16) supplemented with NGF, BDNF, and NT-3 for 48 days (AD, 99–139). Arrows indicate viable neurons that have retained both esterase activity (green cytoplasm) and intact membranes (without red nuclei). d, dendrite; s, synaptic terminal. Roman numerals indicate the cortical layers. Scale bar, 400 μm (*A*); 20 μm (*B–D*); 100 μm (*E*); 35 μm (*G, H*); 400 nm (*F*).

(Fig. 1*B, E*) that were contacted by vesicle-containing synapses (Fig. 1*F*).

Qualitative observations showed that the viability (live/dead stain) of the tissues improved after a few days in vitro vs. that seen directly after chopping. During the first few days, the green cells (containing active esterases) became brighter and the number of red nuclei (dead cells) did not appear to alter. This indicates that the tissue needed to recover from the postmortem situation and the transfer to the culture medium. After recovery, viable cells may be observed after very long periods in vitro (Fig. 1*G, H*). We counted the viable cells (green cytoplasm, dark nucleus), cells with compromised plasma membranes (green cytoplasm, red nucleus), and dead cells (only a red nucleus) in the cortical layers II-VI of slices (n=4/DIV/patient) from three control patients after different periods in culture. The number of viable cortical cells per mm^3 remained relatively constant during the first 2–3 wk (**Fig. 2*A–C***). Since the mean volume of the cortical layers (0.70–0.96 mm^3) in these slices did not change significantly with time in vitro (Fig. 2) it can be concluded that each slice contained many thousands of viable cells during the first weeks in culture. After ~2 wk in vitro, the number of viable cells began to decline significantly in one (Fig. 2*B*) but not in the other two patients (Fig. 2*A, C*). Qualitative observations in tissues taken from seven other patients confirmed that the rate of decline might differ among patients. To what extent this is related to age, disease, pathological hallmarks, postmortem delay, or agonal state at death (16, 17) should be investigated. Qualitative observations (two C and five AD patients) suggested that the addition of a mixture of neurotrophic factors might prolong the viability of the cells (Fig. 1*G, H*). Although the number of dead cells in slices differed among patients and decreased significantly in tissue taken from one patient with time in culture (Fig. 2*C*), an amazingly large number remained present. Consequently, many cells that did not show obvious abnormal morphology in the immunostained slices may well have been dead (cf. Fig. 1*A–D*).

To assess mitochondrial functioning, we used histochemical detection of cytochrome oxidase activity (21, 22), thus enabling localization of active enzyme in all cellular components (neuronal somata, axons, dendrites, glia, and blood vessels) within the tissue. Cytochrome oxidase activity showed an initial recovery effect similar to that observed with the viability staining. For this reason, we began monitoring cytochrome oxidase activity after 1 or more days in vitro. Thereafter, the cytochrome oxidase activity showed a decline whose slope differed among patients (**Fig. 3*A***). Linear regression showed that the slopes were negatively correlated with the age at death of the patients (P=0.01, R^2=0.56), indicating that cytochrome oxidase activity decreased more quickly in cultures taken from older patients. Such a relation was not observed with other clinicopathological characteristics such as disease, postmortem delay, or agonal state at death. To study the

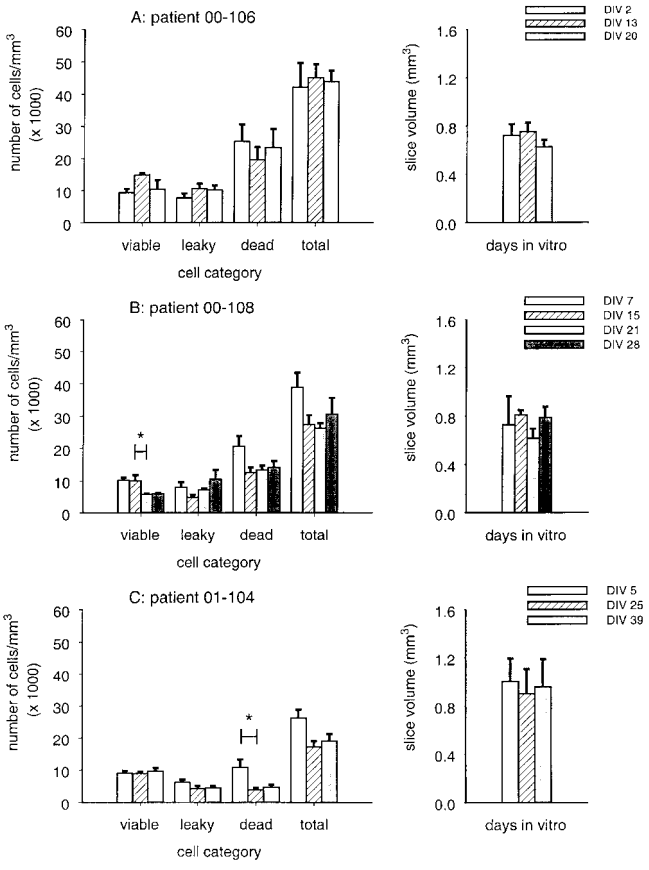

Figure 2. Cell number and volume estimates of slices of three control patients at different times in culture. *A)* In slices from patient (00–106) the volumetric density of all cells (P=0.79), dead cells (P=0.72), leaky cells (P=0.20), and viable cells (P=0.59) remained constant during the first 3 wk. *B)* In slices from patient (00–108) the volumetric density of viable cells decreased significantly during the culture period (P=0.003), whereas the number of all cells (P=0.16), dead cells (P=0.09), and leaky cells (P=0.30) did not show significant changes. *C)* In slices from patient (01–004) the number of dead cells was already low in the first week but declined further during the next 3 wk (P=0.02). This was responsible for a trend in the total number of cells (P=0.05). Viable (P=0.64) and leaky cells (P=0.15) stayed constant. For each patient, the observed changes in the volumes of the cortical layers in the slices were insignificant (right panels). The mean values were 0.70 mm^3 (P=0.72) for patient 00–106, 0.074 mm^3 (P=0.54) for patient 00–108, and 0.96 mm^3 (P=0.85) for patient 01–004, respectively. Asterisks indicate between which time points a significant decrease in the number of the corresponding cell category occurred. The flags denote SE values.

effect of stimulation of mitochondrial metabolism, motor cortex slices from four of the above-mentioned patients (one control, one PD patient, one AD patient, one MS patient) were supplemented with additional pyruvate (final concentration: 2.5 mM; 28). The addition of extra pyruvate significantly delayed the decrease of cytochrome oxidase activity (Fig. 3*B–E*) as indicated by the overall strong interaction between time in vitro and type of medium (P=0.008). We found no indication that diminished mitochondrial functioning was accompanied by extensive cell loss.

Experimental manipulation of neurons with transgenically expressed proteins proved feasible in cultured tissue slices from adult human postmortem brain. After different periods in vitro, slices (total of nine patients, four to nine slices per experiment) were incubated with an rAAV vector containing the LacZ reporter gene (**Fig. 4*A***). In small cells, β-galactosidase activity was limited to the cell body, whereas in large neurons it was also present in the proximal dendrites. To show that cells

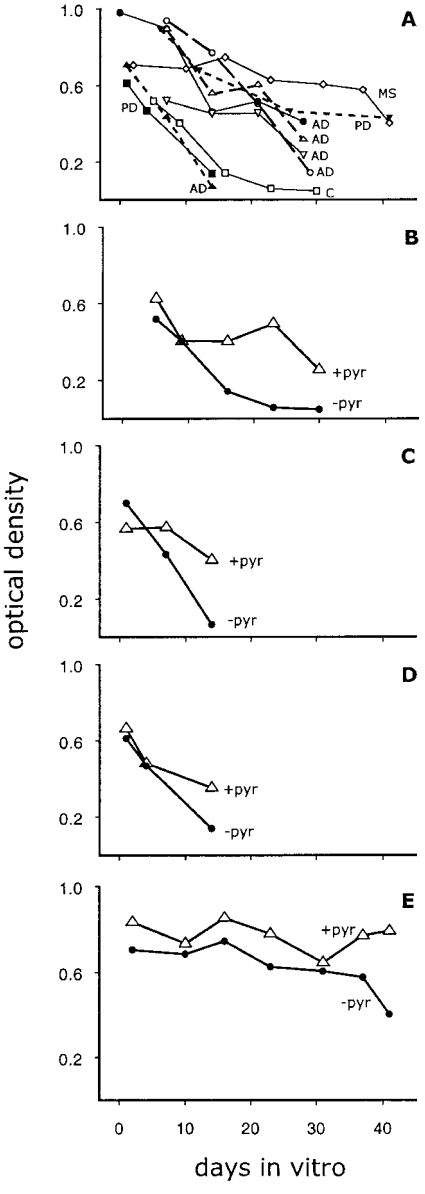

Figure 3. Effect of time in vitro and extra supplementation of pyruvate on cytochrome oxidase activity in layers II and III of motor cortex slices. *A)* Cytochrome oxidase activity declined with different rates in cultures from different patients. Addition of extra pyruvate (+pyr: 2.5 mM pyruvate, −pyr: 0.45 mM pyruvate) delayed the decline of cytochrome oxidase activity in motor cortex slices of a control patient (*B*, 98–143), an AD patient (*C*, 98–111), a PD patient (*D*, 98–140), and an MS patient (*E*, 99–051). The cytochrome oxidase activity is expressed as mean optical density values based on measurements from 2–6 slices per data point. AD: Alzheimer, C: control, MS: multiple sclerosis, PD: Parkinson.

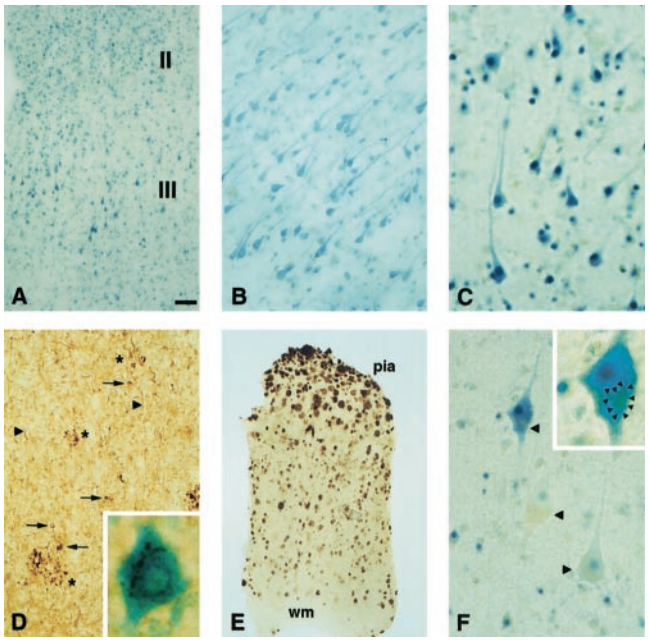

Figure 4. Transgene expression in adult human postmortem brain tissue. *A)* Overview of a motor cortex slice from a control patient showing layers II and III with cells expressing β-galactosidase (patient 99–044, infection at DIV 6; staining at DIV 13; rAAV titer: 8.3×10^8 tu/ml). *B)* Layer III pyramidal neurons of an AD patient (99–001) expressing β-galactosidase at DIV 24 after infection at DIV 14 (rAAV titer: 4.6×10^8 tu/ml). *C)* β-Galactosidase-expressing layer III pyramidal cells in the motor cortex of a PD patient (99–069) (infection at DIV 34; staining at DIV 44; rAAV titer 8.3×10^8 tu/ml). *D)* AT-8 staining at DIV 0 in layer III of a slice from the same tissue block as in panel *B* showing plaques (asterisks), tangles (arrows), and neuropil threads (arrowheads). *D)* Inset: a hyperphosphorylated tau (AT-8) -containing neuron (same patient) that also expressed β-galactosidase (infection at DIV 34; staining at DIV 44; rAAV titer 2×10^8 tu/ml). *E)* Overview of another slice stained at DIV 0 with an antibody against β-amyloid showing the presence of many plaques (same patient as in panel *B*). *F)* Large pyramidal cells of layer V in a motor cortex slice from the same experiment shown in panel *C*. Three adjacent cells suggesting that a high lipofuscin load is accompanied by a low β-galactosidase expression. The inset shows a higher magnification of the uppermost neuron. Arrowheads indicate the location of the lipofuscin accumulations. Scale bar, 400 μm (*E*); 200 μm (*A*); 100 μm (*B, D*); 50 μm (*C, F*); 25 μm (*F,* inset), and 6 μm (*D,* inset).

can express a foreign transgene after being maintained for long periods in vitro, we infected motor cortex slices from an AD patient at DIV 14 (n=8) and a Parkinson patient at DIV 34 (n=5) with an rAAV-LacZ vector (Fig. 4*B, C*). Adjacent slices from the AD patient, stained separately for AD hallmarks, revealed that the area contained many plaques and tangles (Fig. 4*D, E*). Some β-galactosidase-expressing neurons appeared to contain hyperphosphorylated tau deposits (cf. inset Fig. 4*D*). The presence of lipofuscin did not prevent neurons from expressing active β-galactosidase. However, in slices or in areas within slices with many lipofuscin-containing cells, fewer cells expressed β-galactosidase (data not shown) and cells with a relative large amount of lipofuscin showed low β-galactosidase activity (cf. Fig. 4*C, F*). β-Galactosidase activity has never been detected in noninfected slices.

DISCUSSION

Our in vitro approach used tissue slices from postmortem human CNS in which the relative integrity of both microenvironment and cytoarchitecture was maintained. This procedure did not involve dissociation of cells or protease treatment, thereby presumably limiting mechanical damage (loss of axons and dendrites) and impairment of cell surface proteins (receptors, transporters, and ion channels). In such slices, neurons and glial cells retained their cytoarchitectural position and major morphological characteristics, which enabled us to relate their biochemical functioning in vitro to the presence of pathological hallmarks. Extensive dendritic branches and vesicle-containing synaptic terminals also suggested that part of the neuronal network was still present after long-term culturing.

It is generally believed that motor cortex is relatively spared from pathological deposits even in end-stage AD patients (29). We therefore reasoned that motor cortex from control and AD patients would be more comparable than tissue taken from other neocortical areas. Cytochrome oxidase activity measurements appear to corroborate that choice. Although motor cortex slices taken from most AD patients showed substantial pathology, cells in the presence of nearby plaques and neurofibrillary tangles were capable of transgene expression. The β-galactosidase-expressing cells that contained hyperphosphorylated tau might be a target for gene therapy.

The viability and gene transduction experiments showed that many cells in the tissue slices survive the postmortem conditions. The slopes of the cytochrome oxidase activity curves give an impression of the success rate of the cultures taken from different patients. Material from nearly two-thirds of the patients could be used for experiments lasting at least 3 wk, whereas about half of these cultures could be used for more than 30 days. In vitro maintenance was improved by stimulation of the cytochrome oxidase activity using pyruvate, even in tissue from the remaining 1/3 patient group, which survived for less than 2 wk. The positive effect of pyruvate on cytochrome oxidase turnover might occur by shunting glycolysis or, through its role in intracellular calcium homeostasis (28). The mitochondrial functioning in motor cortex cultures appeared to be related to age at the time of death. Aging is accompanied by increased oxidative damage to mitochondrial DNA in the human cerebral cortex (30). It may be that the capacity to survive in vitro is inversely related to the amount of oxidative damage to the mitochondrial DNA. The age of the patients explained 56% (i.e., the coefficient of determination from the linear regression: R^2=0.56) of the variation in the slopes of the cytochrome oxidase activity curves, suggesting there must be other unknown factors. However,

a recent study showed that progenitor cells isolated postmortem from younger individuals survived and proliferated better, corroborating that age is indeed an important factor (31).

Lipofuscin accumulation has been associated with proteolytic dysfunction (32) and lipid peroxidation (33) and may be an early indicator of compromised cellular functions in our slice cultures. Similarly, many dead cells (i.e., with a red nucleus and without active esterases in their cytoplasm) may lack the proteases or the energy necessary for degradation. This would partly explain why the number of dead cells in some tissues remained relatively unchanged during the time in culture. It is unclear why macrophages do not efficiently clear away such neuronal remnants. One implication is that not all cells that can be visualized using immunocytochemical markers are viable. It is interesting that early time-lapse studies conducted on cultures of human brain biopsies reported that the living cells continued migrating out of the explants over long periods (34, 35). This suggests that such cultures were largely composed of dead or moribund tissue that was not degraded. More important, it is unknown whether cell death was due to postmortem delay or dissection and chopping procedures or whether a subset of cells might have perished before the patient died. These possibilities have implications for the interpretation of morphological studies of human postmortem brain where distinguishing healthy from dead cells cannot be accomplished by simple histological evaluation.

In this report, we show that the cells in postmortem brain slices from adult human subjects can be manipulated experimentally and thus can be used for functional studies of human disease processes. FJ

We thank G. Wolswijk, G. J. A. Ramakers, I. Huitinga, and P. Evers for advice, C. J. M. van Ginkel for technical assistance, J. J. van Heerikhuize and C. W. Pool for help with the image analysis, and H. Stoffels, G. van der Meulen, and A. A. Put for photographic expertise. We are grateful to the autopsy team of the Netherlands Brain Bank (coordinator: R. Ravid) for providing us with the brain tissue. This research was partly funded by grants from the Internationale Stichting Alzheimer Onderzoek (ISAO), Alzheimer Stichting Nederland, Platform voor Alternatieven voor Dierproeven, The New Drug Research Foundation, The Research Institute for Diseases in the Elderly (RIDE/NWO), and The Netherlands Organization for Scientific Research (NWO/GB-MW).

REFERENCES

1. Morrison, J. H., and Hof, P. R. (1997) Life and death of neurons in the aging brain. *Science* **278,** 412–419
2. Mrak, R. E., Griffin, S. T., and Graham, D. I. (1997) Aging-associated changes in human brain. *J. Neuropathol. Exp. Neurol.* **56,** 1269–1275
3. Geula, G., Wu, C. K., Saroff, D., Lorenzo, A., Yuan, M., and Yankner, B. A. (1998) Aging renders the brain vulnerable to amyloid β-protein neurotoxicity. *Nature Med.* **4,** 827–831
4. Hardy, J., and Gwinn-Hardy, K. (1998) Genetic classification of primary neurodegenerative disease. *Science* **282,** 1075–1079
5. Price, D. L. (1999) New order from neurological disorders. *Nature (London)* **399,** A3–A5
6. Higgins, L. S., and Cordell, B. (1995) Genetically engineered animal models of human neurodegenerative diseases. *Neurodegeneration* **4,** 117–129
7. Hardy, J. (1999) The shorter amyloid cascade hypothesis. *Neurobiol. Aging* **20,** 85
8. Blass, J. P., and DeGiorgio, L. A. (1992) Tissue culture and studies of human brain disease. *J. Neurol. Sci.* **113,** 1–3
9. Dai, J., Swaab, D. F., and Buijs, R. M. (1998) 'Dead neurons' still have the potential of recovering axonal transport. *Lancet* **351,** 499–500
10. Iqbal, K., and Tellez-Nagel, I. (1972) Isolation of neurons and glial cells from normal and pathological human brains. *Brain Res.* **45,** 296–301
11. Gilden, D. H., Devlin, M., Wroblewska, Z., Friedman, H., Balian-Rorke, L., Santoli, D., and Koprowski, H. (1975) Human brain in tissue culture. I. Acquisition, initial processing, and establishment of brain cell cultures. *J. Comp. Neurol.* **161,** 295–306
12. Kim, S. U., Warren, K. G., and Kalia, M. (1979) Tissue culture of adult human neurons. *Neurosci. Lett.* **11,** 137–141
13. Blass, J. P., Markesby, W. R., Ko, L. W., DeGiorgio, L., Sheu, K. F. R., and Darzynkiewicz, Z. (1994) Presence of neuronal proteins in serially cultured cells from autopsy human brain. *J. Neurol. Sci.* **121,** 132–138
14. McManus, D. Q., and Brewer, G. J. (1997) Culture of neurons from postmortem rat brain. *Neurosci. Lett.* **224,** 193–196
15. Viel, J. J., McManus, D. Q., Cady, G., Evans, M. S., and Brewer, G. J. (2001) Temperature and time interval for culture of postmortem neurons from adult rat cortex. *J. Neurosci. Res.* **64,** 311–321
16. Hardy, J. A., Wester, P., Winblad, B., Gezelius, C., Bring, G., and Erikson, A. (1985) The patients dying after long terminal phase have acidotic brains: implications for biochemical measurements on autopsy tissue. *J. Neural Transm.* **61,** 253–264
17. Ravid, R., van Zwieten, E. J., and Swaab, D. F. (1992) Brain banking and the human hypothalamus—factors to match for, pitfalls and potentials. *Prog. Brain Res.* **93,** 83–95
18. Charpak, S., and Audinat, E. (1998) Cardiac arrest in rodents: maximal duration compatible with a recovery of neuronal activity. *Proc. Natl. Acad. Sci. USA* **95,** 4748–4753
19. Romijn, H. J., de Jong, B. M., and Ruijter, J. M. (1988) A procedure for culturing rat neocortex explants in a serum-free medium. *J. Neurosci. Methods* **23,** 75–83
20. Cragg, B. (1979) Overcoming the failure of electron microscopy to preserve the brain's extracellular space. *Trends Neurosci.* **2,** 159–161
21. Seligman, A. M., Karnovsky, M. J., Wasserkrug, H. L., and Hanker, J. S. (1968) Nondroplet ultrastructural demonstration of cytochrome oxidase activity with a polymerizing osmiophilic reagent, diaminobenzidine (DAB). *J. Cell Biol.* **38,** 1–14
22. Darriet, D., Der, T., and Collins, R. C. (1986) Distribution of cytochrome oxidase in rat brain: Studies with diaminobenzidine histochemistry in vitro and [^{14}C]-cyanide tissue labeling in vivo. *J. Cereb. Blood Flow Metab.* **6,** 8–14
23. Hermens, W. T. J. M. C., ter Brake, O., Dijkhuizen, P. A., Sonnemans, M. A. F., Grimm, D., Kleinschmidt, J. A., and Verhaagen, J. (1999) Purification of recombinant adeno-associated virus by iodixanol gradient ultracentrifugation allows rapid and reproducible preparation of vector stocks for gene transfer in the nervous system. *Hum. Gene Ther.* **10,** 1885–1891
24. Gundersen, H. J. G. (1977) Notes on the estimation of the numerical density of arbitrary profiles: the edge effect. *J. Microsc.* **111,** 219–223
25. Visser, T. D., and Oud, J. L. (1994) Volume measurements in three-dimensional microscopy. *Scanning* **16,** 198–200
26. Verwer, R. W. H., Jansen, K. A., Sluiter, A. A., Pool, C. W., Kamphorst, W., and Swaab, D. F. (2000) Decreased hippocampal metabolic activity in Alzheimer patients is not reflected in the immunoreactivity of cytochrome oxidase subunits. *Exp. Neurol.* **163,** 440–451
27. Pinheiro, J. C., and Bates, D. M. (2000) *Mixed-Effects Models in S and S-PLUS,* Springer, New York
28. Vilalba, M., Martinez-Serrano, A., Gomez-Puertas, P., Blanco, P., Borner, C., Villa, A., Casado, M., Gimenez, C., Pereira, R., Bogonez, E., Pozzan, T., and Sastrustegui, J. (1994) The role of

pyruvate in neuronal calcium homeostasis. *J. Biol. Chem.* **269,** 2468–2476
29. Mesulam, M. M. (1999) Neuroplasticity failure in Alzheimer's disease: bridging the gap between plaques and tangles. *Neuron* **24,** 521–529
30. Mecocci, P., MacGarvey, U., Kaufman, A. E., Koontz, D., Shoffner, J. M., Wallace, D. C., and Beal, M. F. (1993) Oxidative damage to mitochondrial DNA shows marked age-dependent increases in human brain. *Ann. Neurol.* **34,** 609–616
31. Palmer, T. D., Schwartz, P. H., Taupin, P., Kaspar, B., Stein, S. A., and Gage, F. H. (2001) Progenitor cells from human brain after death. *Nature (London)* **411,** 42–43
32. Ezaki, J., Tamida, I., Kanehagi, N., and Kominami, E. (1999) A lysosomal proteinase, the late infantile neuronal ceroid lipofuscinosis gene (*CLN2*) product, is essential for degradation of a hydrophobic protein, the subunit c of ATP synthase. *J. Neurosci.* **72,** 2573–2582
33. Tsai, L., Szweda, P. A., Vinogradova, O., and Szweda, L. I. (2000) Structural characterization and detection of a fluorophore derived from 4-hydroxy-2-noneanal and lysine. *Proc. Natl. Acad. Sci. USA* **95,** 7975–7980
34. Costero, I., and Pomerat, C. M. (1951) Cultivation of neurons from the adult human cerebral and cerebellar cortex. *Am. J. Anat.* **89,** 405–467
35. Hogue, M. J. (1953) A study of adult human brain cells grown in tissue culture. *Am. J. Anat.* **93,** 397–427

Received for publication June 19, 2001.
Revised for publication September 12, 2001.